# Kinetics of exciton photoluminescence in type-II semiconductor superlattices

L. S. Braginsky,* M. Yu. Zaharov, A. M. Gilinsky, V. V. Preobrazhenskii, M. A. Putyato, and K. S. Zhuravlev
*Institute of Semiconductor Physics, 630090 Novosibirsk, Russia*

(Received 1 May 2000; revised manuscript received 8 December 2000; published 12 April 2001)

The exciton decay rate at a rough interface in type-II semiconductor superlattices is investigated. It is shown that the possibility of recombination of the indirect excitons at a plane interface essentially affects the kinetics of the exciton photoluminescence at a rough interface. This is the result of the quantum interference of electrons scattered from the plane interface and at the roughnesses. Expressions that relate the parameters of the luminescence kinetics with the statistical characteristics of the rough interface are obtained. The mean height and length of the roughnesses in GaAs/AlAs superlattices are estimated from the experimental data.

DOI: 10.1103/PhysRevB.63.195305 PACS number(s): 78.66.Fd

## I. INTRODUCTION

GaAs/AlAs type-II superlattices are the subjects of extensive investigation in the recent decade. Electrons and holes are separated in these structures: the holes are confined in the $\Gamma$ valley of GaAs, whereas the electrons are in the $X$ valleys of AlAs. Changing the width of the AlAs layer during the structure growth, it is possible to confine the electrons either in the $X_z$ valley (the $X$ valley that is directed along the structure axis [001]) or in the $X_{xy}$ valley (the $X$ valley that is directed along the GaAs/AlAs interface: [100] or [010]). The excitons in such structures are indirect in both the real and momentum spaces.

The kinetics of exciton luminescence is usually investigated experimentally by the time-resolved method. The theory by Klein *et al.*[1] is commonly used to explain the results of such experiments. This theory has been developed to consider the no-phonon radiative decay rates of indirect excitons in alloy semiconductors (e.g., $Ga_{1-x}Al_xAs$). The recombination of indirect excitons occurs because of intervalley scattering of electrons at the potential fluctuations caused by the compositional disorder. These short-range scatterers are necessary to compensate for the large momentum of an electron in the $X$ valley. The nonexponential time dependence of the decay rate has been obtained

$$I(t) \propto e^{-w_0 t}(1+2w_r t)^{-3/2}, \tag{1}$$

where the value $w_r$ is connected with the compositional disorder. The exponential factor has been included in Eq. (1) to consider different nonstochastic processes of the exciton recombination (e.g., phonon-assisted recombination); $w_0$ is the decay rate resulted from all nonstochastic processes. This is possible only in the absence of any correlation between the stochastic and nonstochastic processes.

The possibility of applying the theory of Ref. 1 to superlattices has been discussed by Minami *et al.*[2] The authors suppose that short-range scatterers are distributed along the plane boundary. This assumption justifies the application of Eq. (1) for superlattices; however, it does not allow us to relate the parameter $w_r$ with the characteristics of the rough interface, e.g., the mean height and length of the roughness. Krivorotov *et al.*[3] have shown that nonradiative decay due to exciton trapping by interfacial defects also leads to a nonexponential factor in Eq. (1). Nevertheless, Eq. (1), wherein the parameters $w_r$ and $w_0$ are considered as trial, is commonly used for analysis of the experimental results.[4]

It should be noted that the presence of the interface roughness is not necessary for the recombination of $X_z$ excitons. Their recombination occurs even at a plain interface where the normal component of the electron momentum relaxes. This important point also distinguishes the exciton recombination in superlattices. The process, however, cannot be taken into account by a simple exponential factor. Indeed, the wave function of the electron at a rough interface is the sum of its regular and diffuse components. The regular part exists at a plane interface, whereas the diffuse one is due to the roughness. As a result the crossed terms, which mix these components, arise in the interband matrix element; so that the probability of the exciton recombination, which is determined by the squared module of this matrix element, is no longer a simple sum of the probabilities of the recombination at the plane interface and at the roughness. This correlation leads to a more complicated relation than the simple exponential factor in Eq. (1).

In this paper we consider a more realistic model of a rough interface. We show that Eq. (1) holds for the decay rate of $X_{xy}$ excitons and we relate the $w_r$ value with the parameters of the rough interface. We determine the decay rate of $X_z$ excitons. In particular, it is found that this value at large delay times behaves roughly as $I(t) \propto \exp(-w_0 t)/t$, rather than $I(t) \propto \exp(-w_0 t)/t^{3/2}$ as is predicted by Eq. (1). Our experiments on GaAs/AlAs type-II superlattices confirm these results. We use the experimental data for the radiative decay rates to estimate the parameters of the rough interface. The mean height of roughnesses was found to be close to the lattice constant, whereas their mean length is about 50 Å .

## II. RADIATIVE DECAY RATES OF INDIRECT EXCITONS IN SUPERLATTICES THEORY

Let $z=0$ be the interface between GaAs ($-d_1<z<0$) and AlAs ($0<z<d_2$), and $\boldsymbol{\rho}$ be the vector in the $XY$ plane. We consider the exiton recombination at the interface and write the exciton wave function as follows:[5]

$$\phi(\mathbf{r}_e, \mathbf{r}_h) = f_e(z_e) f_h(z_h) G(\boldsymbol{\rho}_e - \boldsymbol{\rho}_h, z_e, z_h),$$

 

where $\mathbf{r}_e=\{\boldsymbol{\rho}_e,\ z_e\}$ and $\mathbf{r}_h=\{\boldsymbol{\rho}_h,\ z_h\}$ are the coordinates of the electron and the hole, and $f_e(z_e)$ and $f_h(z_h)$ are their wave functions in the absence of Coulomb interaction; the function $G$ takes into account this interaction. The probability of the exciton recombination is proportional to $G^2(\mathbf{0})$ $[G(\mathbf{0})\equiv G(\boldsymbol{\rho}_e=\boldsymbol{\rho}_h, z_e=z_h=0)]$ and the squared module of the matrix element

$$\mathcal{P}=\int f_e(z)\nabla f_h(z)\,dz\,d^2\boldsymbol{\rho}. \tag{2}$$

The functions $f_e(z_e)$ and $f_h(z_h)$ can be expressed via the envelope wave functions of the electron and the hole in the conduction and valence bands of GaAs and AlAs. To determine the envelopes, the appropriate boundary conditions at the GaAs/AlAs interface should be imposed. The roughness of the interface has an influence on these boundary conditions and, therefore, affects the envelopes. We shall consider the rough interface where the mean height of the roughnesses is small in comparison with the electron wavelength (or the exciton Bohr radius). This allows us to use the boundary conditions at the rough interface[6] to consider the influence of the roughness on the exciton recombination. In addition, this allows us to neglect the effect of the roughness on the function $G$.

### A. Boundary conditions for the envelope wave functions at a GaAs/AlAs interface

#### 1. Boundary conditions at a plane interface

In general, the boundary conditions for the electron envelopes can be written as follows:

$$\begin{pmatrix} \Psi^r_\Gamma \\ \partial_z\Psi^r_\Gamma \\ \Psi^r_{Xxy} \\ \partial_z\Psi^r_{Xxy} \\ \Psi^r_{Xz} \\ \partial_z\Psi^r_{Xz} \end{pmatrix} = \tilde{T}\begin{pmatrix} \Psi^l_\Gamma \\ \partial_z\Psi^l_\Gamma \\ \Psi^l_{Xxy} \\ \partial_z\Psi^l_{Xxy} \\ \Psi^l_{Xz} \\ \partial_z\Psi^l_{Xz} \end{pmatrix}, \tag{3}$$

where $\Psi^{l,r}_{\Gamma,Xxy,Xz}$ are the envelopes which correspond to the $\Gamma$, $X_{xy}$, and $X_z$ valleys of GaAs and AlAs; $\partial_z\Psi^{l,r}_{\Gamma,Xxy,Xz}\equiv\partial\Psi^{l,r}_{\Gamma,Xxy,Xz}/\partial z$ are their normal derivatives. The elements $\tilde{t}_{ik}$ of the $6\times6$ matrix $\tilde{T}$ are determined by the interface structure. They are independent of the electron energy. For the GaAs/$Al_xGa_{1-x}$As interface they have been calculated by Ando and Akera.[7]

We shall consider the particular cases of $X_z$ and $X_{xy}$ excitons. This allows us to simplify Eq. (3). First, we omit mixing between $X_z$ and $X_{xy}$ valleys. Second, the energy position of the $\Gamma$ minimum in AlAs is considerably higher than that of the $X$ minimum. For this reason the wave function $\Psi^r_\Gamma$ decays rapidly away from the interface. We have $\Psi^r_\Gamma \propto\exp(-\gamma^r z)$, $\partial_z\Psi^r_\Gamma=-\gamma^r\Psi^r_\Gamma$, where $\gamma^r=\sqrt{2m^r_\Gamma(E_\Gamma-\varepsilon_e)}$ (here $m^r_\Gamma$ is effective mass in the $\Gamma$ valley of AlAs, $\varepsilon_e\approx E_X$ is the electron energy, $E_\Gamma$ and $E_X$ are the energies of the bottoms of the $\Gamma$ and $X$ valleys) can be considered as independent of the electron energy. By elimination of $\partial_z\Psi^r_\Gamma$ from Eq. (3), for the $X_z$ electrons we find

$$\Psi^r_{Xz}=\Psi^l_{Xz}, \tag{4a}$$

$$\partial_z\Psi^r_{Xz}=t^z_{41}\partial_z\Psi^l_\Gamma+t^z_{44}\partial_z\Psi^l_{Xz},$$

$$\Psi^l_\Gamma+t^z_{12}\partial_z\Psi^l_\Gamma+t^z_{13}\Psi^l_{Xz}=0,$$

where $t^z_{44}\approx m^r_{Xl}/m^l_{Xl}\approx1$; this value takes into account the difference in longitudinal effective masses in the $X$ valleys of AlAs and GaAs; $t^z_{41}=t_{\Gamma X}m^r_{Xl}/(m_e a)$, $t^z_{12}=m^r_\Gamma/(m^l_\Gamma\gamma^r)$, $t^z_{13}=t_{\Gamma X}m^l_\Gamma/(m_e a\gamma^r)\ll1$; $m^{l,r}_\Gamma$ are electron effective masses in the $\Gamma$ valleys of AlAs and GaAs, $t_{\Gamma X}\approx1$ is the parameter of $\Gamma$-$X$ mixing, $m_e$ is mass of the free electron, and $a$ is the lattice constant. Other elements of the $t^z_{ik}$ matrix are small; this is the result of numerical calculations of Ref. 7.

Note that the band states in the $X$ valley result from the interaction of two close-lying bands: the lower $X_1$ and upper $X_3$; meanwhile only the $X_3$ states mix efficiently with $\Gamma$ states. This means that $t_{\Gamma X}\approx1$ is the upper estimation of $\Gamma$-$X$ mixing.

It is sufficient to consider only the $X$ valleys of each contacting material when $X_{xy}$ electrons are considered. Assuming $\partial_z\Psi^l_\Gamma=\gamma^l\Psi^l_\Gamma$, where $\gamma^l\sim2\pi/a$, from Eq. (3) we find

$$\Psi^r_{Xxy}=t^{xy}_{11}\Psi^l_{Xxy}+t^{xy}_{12}\partial_z\Psi^l_{Xxy}, \tag{4b}$$

$$\partial_z\Psi^r_{Xxy}=t^{xy}_{21}\Psi^l_{Xxy}+t^{xy}_{22}\partial_z\Psi^l_{Xxy},$$

where $|t^{xy}_{12}|\ll1$, $|t^{xy}_{21}|\ll a^{-1}$, $t^{xy}_{11}\approx1$, and $t^{xy}_{22}\approx m^r_{Xt}/m^l_{Xt}\approx1$; $m^r_{Xt}$ and $m^l_{Xt}$ are the transversal effective masses of AlAs and GaAs.

The bands of the light and heavy holes are split due to the size quantization. This allows us to consider only the heavy holes in each material and write the boundary conditions for them as follows:

$$\Psi^r_h=t^h_{11}\Psi^l_h+t^h_{12}\partial_z\Psi^l_h, \tag{4c}$$

$$\partial_z\Psi^r_h=t^h_{21}\Psi^l_h+t^h_{22}\partial_z\Psi^l_h,$$

where $\Psi^{l,r}_h$ are the envelopes for the heavy holes in each material; $t^h_{11}\approx1$, $t^h_{22}\approx m^r_{hh}/m^l_{hh}$, $|t^h_{12}|\ll1$, $|t^h_{21}|\ll a^{-1}$, and $m^{l,r}_{hh}$ are the longitudinal effective masses of the heavy holes.

#### 2. Boundary conditions at a rough interface

We shall consider the model of a rough interface that is schematically drawn in Fig. 1. This model is in agreement with the optical[8] and structural[9] investigations of the GaAs/AlAs interface. The interface looks like the array of the plane areas of the same crystallographic orientation. The random function $z=\xi(\boldsymbol{\rho})$ of the coordinates in the $XY$ plane determines the positions of these areas relative to $z=0$.

We assume the average height of roughnesses $h$ to be small in comparison with the electron wavelength. Then it is possible to describe the rough interface by means of a cor-

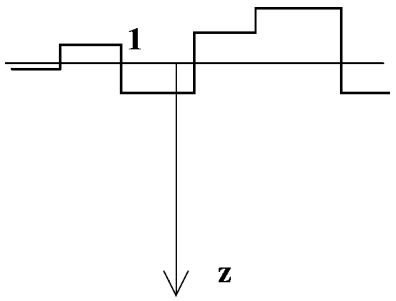


FIG. 1. The model of the rough interface: side view.

relation function $W(\boldsymbol{\rho},\boldsymbol{\rho}'')=\overline{\xi(\boldsymbol{\rho})\xi(\boldsymbol{\rho}'')}$. For a homogeneous rough interface $W(\boldsymbol{\rho},\boldsymbol{\rho}'')=W(\boldsymbol{\rho}-\boldsymbol{\rho}'')$, i.e., the correlation function is the function of a one vector variable: $\boldsymbol{\rho}=\boldsymbol{\rho}-\boldsymbol{\rho}''$. There are two parameters that are most important when the statistical properties of a rough interface are considered: $h^2=W(0)$, and the correlation length $l$, which is the mean attenuation length of the correlation function. In our model the correlation length can be associated with the mean size of the plane area.

The special form of the rough interface (Fig. 1) allows us to apply the boundary conditions (4), which are applicable at a plane interface, at each plane $z=\xi$. The inequality $|\xi\partial_z\Psi|\sim h/\lambda\ll 1$ ($\lambda$ is the electron wavelength) allows us to rewrite these boundary conditions at a plane $z=0$. After some algebra (see Appendix A), we obtain

$$\Psi^r_{Xz}=-t^z_{41}\eta(\xi)\xi(\boldsymbol{\rho})\Psi^l_\Gamma+\Psi^l_{Xz}+(1-t^z_{44})\xi(\boldsymbol{\rho})\partial_z\Psi^l_{Xz}, \tag{5a}$$

$$\partial_z\Psi^r_{Xz}=t^z_{41}\eta(\xi)\Psi^l_\Gamma+t^z_{41}\eta(\xi)\xi(\boldsymbol{\rho})\Psi^l_\Gamma+t^z_{44}\partial_z\Psi^l_{Xz},$$

$$\Psi^l_\Gamma+[t^z_{12}+\xi(\boldsymbol{\rho})]\partial_z\Psi^l_\Gamma+t^z_{13}\eta^*(\xi)\Psi^l_{Xz}$$

$$+t^z_{13}\eta^*(\xi)\xi(\boldsymbol{\rho})\partial_z\Psi^l_{Xz}=0$$

for the electrons in the $X_z$ valley,

$$\Psi^r_{Xxy}=\Psi^l_{Xxy}+(1-t^{xy}_{22})\xi(\boldsymbol{\rho})\partial_z\Psi^l_{Xxy}, \tag{5b}$$

$$\partial_z\Psi^r_{Xxy}=t^{xy}_{21}\Psi_{Xxy}+t^{xy}_{22}\partial_z\Psi^l_{Xxy}$$

for the electrons in the $X_{xy}$ valley, and

$$\Psi^r_h=\Psi^l_h+(1-t^h_{22})\xi(\boldsymbol{\rho})\partial_z\Psi^l_h, \tag{5c}$$

$$\partial_z\Psi^r_h=t^h_{21}\Psi_h+t^h_{22}\partial_z\Psi^l_h$$

for the holes. Factor $\eta(\xi)=\exp(2\pi i\xi/a)$ in Eq. (5a) takes two values $\pm 1$ for $\xi=a$ or $\xi=a/2$, respectively. It has been introduced in Ref. 10 to take into account the symmetry properties of the Bloch functions with respect to translation by a single monomolecular layer ($a/2$) along the $z$ axis. The Bloch function of the electron in the $X_z$ valley changes its sign under this translation whereas the Bloch function of the electron in the $\Gamma$ valley does not. Therefore, the parameter $t_{\Gamma X}$ of $\Gamma$-$X$ mixing also should change sign under such translation. This is not important at a plane interface, but must be taken into account when the relative positions of some interfaces are considered. We assume $|t^{xy,h}_{21}|\ll a^{-1}$: this is the result of numerical calculations of Ref. 7.

Unlike Eqs. (4) the boundary conditions (5) contain the terms that depend on $\xi$. They would not be important if $\xi=$const. Then they are relevant to the phase shift of the wave functions arisen from the shift of the interface. However, these terms become important when $\xi$ depends on $\boldsymbol{\rho}$. The interference of the electrons scattered from the neighboring planes in the vicinity of steps (like point 1 in Fig. 1) results in the appearance of the diffuse components of their wave functions. The mean size of the region at the step where the interference occurs is the parallel-to-interface component of the electron wavelength. Hence the ratio of this size to the size of the plane area $l$ characterizes the roughnesses influence on the electrons.

We separate the diffuse components $\varphi^{l,r}_{\Gamma,X_z,X_{xy}}$ of the envelope wave functions and write the envelopes as follows:[11]

$$\Psi^{l,r}_{\Gamma,X_z,X_{xy}}=\Phi^{l,r}_{\Gamma,X_z,X_{xy}}+\varphi^{l,r}_{\Gamma,X_z,X_{xy}}, \quad \text{where} \quad \overline{\varphi^{l,r}_{\Gamma,X_z,X_{xy}}}=0. \tag{6}$$

Using the boundary conditions (5), for the envelopes $\Phi^{l,r}_{\Gamma,X_z,X_{xy}}$ and $\varphi^{l,r}_{\Gamma,X_z,X_{xy}}$ (see Appendix B for details), we obtain

$$\Phi^l_\Gamma(\mathbf{r})=T_\Gamma e^{-ip_\Gamma z},$$

$$\Phi^l_{X_z,X_{xy}}(\mathbf{r})=T_{X_z,X_{xy}}e^{\gamma_{X_z,X_{xy}}z},$$

$$\Phi^r_{X_z,X_{xy}}(\mathbf{r})=e^{-iqz}+R_{X_z,X_{xy}}e^{iqz},$$

$$\Phi^l_h(\mathbf{r})=e^{ipz}+R_he^{-ipz}, \quad \Phi^r_h(\mathbf{r})=T_he^{-\gamma_hz},$$

$$\varphi^l_\Gamma(\mathbf{r})=\frac{2q}{(2\pi)^2}\int_{-\infty}^{\infty}A^l_\Gamma(\boldsymbol{k}_\parallel)\tilde{\xi}(\boldsymbol{k}_\parallel)e^{i(\mathbf{k}\cdot\boldsymbol{\rho}-k_\Gamma z)}\,d\boldsymbol{k}_\parallel, \tag{7}$$

$$\varphi^l_{X_z,X_{xy}}(\mathbf{r})=\frac{2q}{(2\pi)^2}\int_{-\infty}^{\infty}A^l_{X_z,X_{xy}}(\boldsymbol{k}_\parallel)\tilde{\xi}(\boldsymbol{k}_\parallel)e^{i\mathbf{k}\cdot\boldsymbol{\rho}+\varkappa_{\Gamma,X_z,X_{xy}}z}\,d\boldsymbol{k}_\parallel,$$

$$\varphi^r_{X_z,X_{xy}}(\mathbf{r})$$

$$=\frac{2q}{(2\pi)^2}\int_{-\infty}^{\infty}A^r_{\Gamma,X_z,X_{xy}}(\boldsymbol{k}_\parallel)\tilde{\xi}(\boldsymbol{k}_\parallel)e^{i(\mathbf{k}\cdot\boldsymbol{\rho}+k_{X_z,X_{xy}}z)}\,d\boldsymbol{k}_\parallel,$$

$$\varphi^l_h(\mathbf{r})=\frac{2p}{(2\pi)^2}\int_{-\infty}^{\infty}A^l_h(\boldsymbol{k}_\parallel)\tilde{\xi}(\boldsymbol{k}_\parallel)e^{i(\mathbf{k}\cdot\boldsymbol{\rho}-k_hz)}\,d\boldsymbol{k}_\parallel,$$

$$\varphi^r_h(\mathbf{r})=\frac{2p}{(2\pi)^2}\int_{-\infty}^{\infty}A^r_h(\boldsymbol{k}_\parallel)\tilde{\xi}(\boldsymbol{k}_\parallel)e^{i\mathbf{k}\boldsymbol{\rho}-\varkappa_hz}\,d\boldsymbol{k}_\parallel,$$

where

$$k_\Gamma(\boldsymbol{k}_\parallel)=\sqrt{2m_\Gamma(\varepsilon_e-E^l_\Gamma)-\boldsymbol{k}^2_\parallel},$$

$$\varpi_{X_z}(\boldsymbol{k}_\parallel)=\sqrt{2m^l_{Xl}(E^l_{X_z}-\varepsilon_e)+\boldsymbol{k}^2_\parallel},$$

$$\varpi_{X_{xy}}(\boldsymbol{k}_\parallel)=\sqrt{2m^l_{Xt}(E^l_{X_{xy}}-\varepsilon_e)+\boldsymbol{k}^2_\parallel},$$

$$k_{X_z}(\boldsymbol{k}_\parallel)=\sqrt{2m^r_{Xl}(\varepsilon_e-E^r_{X_z})-\boldsymbol{k}^2_\parallel},$$

$$k_{X_{xy}}(\boldsymbol{k}_\parallel)=\sqrt{2m^r_{Xt}(\varepsilon_e-E^r_{X_{xy}})-\boldsymbol{k}^2_\parallel},$$

$$k_h(\boldsymbol{k}_\parallel)=\sqrt{2m^l_h(E^l_h-\varepsilon_h)-\boldsymbol{k}^2_\parallel},$$

$$\varpi_h(\boldsymbol{k}_\parallel)=\sqrt{2m^r_h(\varepsilon_h-E^r_h)+\boldsymbol{k}^2_\parallel}, \quad \mathrm{Im}\, k_{X_z,X_{xy},h}\geqslant 0,$$

$$T_\Gamma=\frac{2iqt^z_{13}\eta(\xi)}{t^z_{44}\gamma_{X_z}}, \quad T_{X_z}=-\frac{2iq}{t^z_{44}\gamma_{X_z}}, \quad R_{X_z}=-1-\frac{2iq}{t^z_{44}\gamma_{X_z}},$$

$$T_{X_{xy}}=\frac{2iq}{t^{xy}_{21}+t^{xy}_{22}\gamma_{X_{xy}}}, \quad R_{X_{xy}}=-1+\frac{2iq}{t^{xy}_{21}+t^{xy}_{22}\gamma_{X_{xy}}},$$

$$T_h=-\frac{2ip}{-t^h_{21}+t^h_{22}\gamma_h}, \quad R_h=-1-\frac{2ip}{-t^h_{21}+t^h_{22}\gamma_h},$$

$$A^l_\Gamma=\frac{it^z_{13}\eta(\xi)}{t^z_{44}}, \quad A^r_{X_z}=-\frac{i}{t^z_{44}}\left(\frac{t^z_{13}t^z_{41}}{\gamma_{X_z}}+1-t^z_{44}\right),$$

$$A^l_{X_z}=-\frac{k_{X_z}}{\varpi_{X_z}{t^z_{44}}^2}\left(\frac{t^z_{13}t^z_{41}}{\gamma_{X_z}}+1-t^z_{44}\right),$$

$$A^r_{X_{xy}}=i\frac{t^{xy}_{22}\varpi_l\varpi_{X_{xy}}(1-t^{xy}_{22})}{(t^{xy}_{21}+\varpi_{X_{xy}}t^{xy}_{22})(t^{xy}_{22}\varpi_l+ik_{X_{xy}})},$$

$$A^l_{X_{xy}}=k_z\frac{\varpi_{X_{xy}}(1-t^{xy}_{22})}{(t^{xy}_{21}+\varpi_{X_{xy}}t^{xy}_{22})(t^{xy}_{22}\varpi_l+ik_{X_{xy}})},$$

$$A^r_h=-\frac{k_h(1-t^h_{22})}{t^h_{22}(\varpi_h t^h_{22}-t^h_{21})}, \quad A^l_h=i\frac{\varpi_h(1-t^h_{22})}{\varpi_h t^h_{22}-t^h_{21}}.$$

Here $\tilde{\xi}(\boldsymbol{k}_\parallel)=\int\xi(\boldsymbol{\rho})e^{-i\mathbf{k}\cdot\boldsymbol{\rho}}d\boldsymbol{\rho}$, $\gamma_{X_z,X_{xy},h}=\varpi_{X_z,X_{xy},h}(0)$, $p_\Gamma=k_\Gamma(0)$; $E^l_\Gamma$, $E^l_{X_z}$, $E^l_{X_{xy}}$, $E^r_{X_z}$, $E^r_{X_{xy}}$, $E^l_h$, and $E^r_h$ are the energies of the extrema of the appropriate bands. The integration in Eq. (7) is carried out over the whole plane, because $\xi(\boldsymbol{\rho})$ is not a periodical function of $\boldsymbol{\rho}$. The values of normal-to-interface components of the wave vectors of the electrons $q$ and holes $p$ are determined by the boundary conditions at the interfaces: $z=-d_1$ for $p$ and $z=d_2$ for $q$ (where $d_1$ and $d_2$ are the widths of GaAs and AlAs layers). In general, they depend on the valley under consideration: $\tan(qd_2/2)=-(q/\gamma_{X_z})$ for the electrons in the $X_z$ valley, $\tan qd_2=-2q/(t^{xy}_{22}\gamma_{X_{xy}}+t^{xy}_{21})$ for the electrons in the $X_{xy}$ valley, and $\tan pd_1=-2p/(t^h_{22}\gamma_h-t^h_{21})$ for the holes. We assume, however, the strong confinement of electrons and holes in the appropriate layers $\gamma_{X_z,X_{xy},h}\gg p,q$, so that $p\approx\pi/d_1$ and $q\approx\pi/d_2$.

The wave vector of the electron in the GaAs $\Gamma$ valley is small, $p_\Gamma\ll p$; nevertheless, it is real. This distinguishes the short-period GaAs/AlAs superlattices from other type-II structures, where the electron wave function decays rapidly away from the interface. The electron density is large in AlAs and small, but almost constant, in GaAs. This small part of the electron density could be essential for the exiton recombination would the effective parameter of $\Gamma$-$X$ mixing $t^z_{13}$ be sufficiently large.

### B. Radiative decay rates of indirect excitons at a rough interface

To determine the wave functions $f_e(z)$ and $f_h(z)$, we have to insert the corresponding Bloch amplitudes into expressions for the envelopes $\Psi_e$ and $\Psi_h$ (6). For instance, for the $X_z$ exciton at a plane interface, we have

$$f_e(\mathbf{r})=\frac{1}{\sqrt{N_1}}\begin{cases}T_\Gamma u_\Gamma(\mathbf{r})e^{\gamma_\Gamma z}+T_{X_z}u_X(\mathbf{r})e^{[\gamma_{X_z}-(2\pi i/a)]z}, & z<0\\ u^*_X(\mathbf{r})e^{i[q-(2\pi i/a)]z}+R_{X_z}u_X(\mathbf{r})e^{-i[q-(2\pi i/a)]z}, & z>0,\end{cases} \tag{8}$$

$$f_h(\mathbf{r})=\frac{1}{\sqrt{N_2}}\begin{cases}v(\mathbf{r})e^{ipz}+R_hv^*(\mathbf{r})e^{-ipz}, & z<0\\ T_hv(\mathbf{r})e^{-\gamma_h z}, & z>0,\end{cases}$$

where $N_1$ and $N_2$ are the numbers of atoms in the AlAs and GaAs layers, respectively, $u_\Gamma(\mathbf{r})$, $u_X(\mathbf{r})$, and $v(\mathbf{r})$ are the Bloch amplitudes of the electrons in the $\Gamma$ and $X$ valleys, and the holes; we assume these amplitudes to be periodical functions of $\mathbf{r}$.

At a rough interface we have to add also the diffuse components of the wave functions. To do that, we have to multiply $\varphi(\mathbf{r})$ (7) by the corresponding Bloch amplitudes. Usually the mean size of the Bloch amplitudes is small in comparison with the lattice constant. This allows us to assume that the $\boldsymbol{\nabla}$ operator in Eq. (2) acts only on these amplitudes and to separate the integration of them from the integration of the envelopes. Then the matrix element (2) can be written as $\mathcal{P}=\mathcal{P}_1+\mathcal{P}_2+\mathcal{P}_3$, where

$$\mathcal{P}_1=\sum_{\Gamma,X}U_{\Gamma,X}\int\Phi_{\Gamma,X_z,X_{xy}}\Phi_h\,dz\,d\boldsymbol{\rho}, \tag{9}$$

$$\mathcal{P}_2=\sum_{\Gamma,X} U_{\Gamma,X}\int [\Phi_{\Gamma,X_z,X_{xy}}\varphi_h+\Phi_h\varphi_{\Gamma,X_z,X_{xy}}]\,dz\,d\boldsymbol{\rho},$$

$$\mathcal{P}_3=\sum_{\Gamma,X} U_{\Gamma,X}\int \varphi_{\Gamma,X_z,X_{xy}}\varphi_h\,dz\,d\boldsymbol{\rho}.$$

Here $\Phi=\Phi^l$, $\varphi=\varphi^l$ if $z<\xi$; $\Phi=\Phi^r$, $\varphi=\varphi^r$ if $z>\xi$; $U_\Gamma=\Omega_0^{-1}\int_{\Omega_0}u_\Gamma(\mathbf{r})\boldsymbol{\nabla}v(\mathbf{r})\,d\mathbf{r}$, $U_X=\Omega_0^{-1}\int_{\Omega_0}u_X(\mathbf{r})\boldsymbol{\nabla}v(\mathbf{r})\,d\mathbf{r}$, and $\Omega_0$ is the unit cell.

The rate of the exciton recombination is

$$w=\Lambda(|\mathcal{P}_1|^2+\mathcal{P}_1\mathcal{P}_2^*+\mathcal{P}_1^*\mathcal{P}_2+\mathcal{P}_1\mathcal{P}_3^*+\mathcal{P}_1^*\mathcal{P}_3+|\mathcal{P}_2|^2), \tag{10}$$

$$\Lambda=\frac{4\hbar e^2\omega}{3m_e^2c^3}G^2(\mathbf{0}),$$

where $\hbar\omega$ is the exciton energy, and $e$, $m_e$, and $c$ are the fundamental constants.

The luminescence intensity $I(t)$ is proportional to the recombination rate $w$ and the number of excitons at the time $t$. We assume this number to be proportional to $\exp(-wt)$ (or $\exp[-(w_0+w)t]$, if some nonstochastic process with the rate $w_0$ occurs). The $w$ value is stochastic, since it depends on $\xi$. Therefore, to determine the luminescence intensity, we have to average the value of $w\exp(-wt)$ over the realization of the random function $\xi$. This can be done if we know the distribution $P(w)$ of the $w$ value: $\overline{w\exp(-wt)}=\int_0^\infty w\exp(-wt)P(w)\,dw$. The distribution $P(w)$ essentially depends on $\mathcal{P}_1$, whether or not it vanishes.

If $\mathcal{P}_1=0$ (i.e., if the exciton recombination at a plane interface is forbidden) then $w$ is proportional to the squared module of $\mathcal{P}_2$. The linear relationship between $\mathcal{P}_2$ and the random variable $\xi$ follows from Eqs. (7) and (9). Therefore, if the distribution of $\xi$ is Gaussian, then the distribution of $\mathcal{P}_2$ is also Gaussian and the distribution of $w$ is exponential. This means that the arguments of Refs. 1 and 2 hold, so that $I(t)$ is determined by Eq. (1) where $w_r=\Lambda|\mathcal{P}_2|^2$. For the case of the $X_{xy}$ exciton we have

$$\mathcal{P}_2=\frac{4pqU_X}{\sqrt{N_1N_2}}\sum_{\mathbf{g}}\left[\frac{1-t_{22}^h}{\gamma_{X_{xy}}^2}\tilde{\xi}(\mathbf{q}_X+\mathbf{g})+\frac{1-t_{22}^{xy}}{\gamma_h^2}\tilde{\xi}^*(\mathbf{q}_X+\mathbf{g})\right],$$

and

$$w_r=\frac{16\pi^4a^4|U_X|^2\Lambda}{d_1^3d_2^3}\left[\frac{(1-t_{22}^h)^2}{\gamma_{X_{xy}}^4}+\frac{(1-t_{22}^{xy})^2}{\gamma_h^4}\right]\tilde{W}\left(\frac{2\pi}{a}\right), \tag{11}$$

where $\tilde{W}(\mathbf{k})=\int W(\boldsymbol{\rho})e^{-ik\rho}\,d^2\boldsymbol{\rho}$ is the Fourier transform of the correlation function, $\mathbf{q}_X=\{2\pi/a,0,0\}$ is the wave vector of the $X$ valley, and $\mathbf{g}$ is the two-dimensional reciprocal-lattice vector; it arises here since the integration in Eq. (7) has not been restricted by the first Brillouin zone.

If $\mathcal{P}_1\neq0$ (i.e., if the exciton recombination at a plane interface is allowed) then the linear terms with respect to $\mathcal{P}_2$ in Eq. (10) are nonzero. This allows us to omit the terms with $\mathcal{P}_3$ and $|\mathcal{P}_2|^2$, which are quadratic in $\xi$, or replace them with their average values. Then $w$ becomes the linear function of the random variable $\xi$. If the distribution of $\xi$ is Gaussian then the distribution of $w$ is Gaussian too, i.e.,

$$P(w)=\frac{1}{\sigma\sqrt{2\pi}}e^{-[(w-\bar{w})^2/2\sigma^2]},$$

where $\bar{w}=\Lambda|\mathcal{P}_1|^2$ and $\sigma=[\overline{|w-\bar{w}|^2}]^{1/2}$. Hence

$$I(t)=\frac{e^{-w_0t}}{\sigma\sqrt{2\pi}}\int_0^\infty we^{-wt-[(w-\bar{w})^2/2\sigma^2]}\,dw=e^{-(\bar{w}+w_0)t}\times\left[\frac{\sigma}{\sqrt{2\pi}}+\frac{\bar{w}-\sigma^2t}{2}e^{(\sigma^2t^2/2)}\mathrm{erfc}\left(\frac{\sigma t}{\sqrt{2}}\right)\right]. \tag{12}$$

If $|\mathcal{P}_1|\gg|\mathcal{P}_2|$, then $\sigma^2\simeq2\Lambda^2|\mathcal{P}_1|^2\overline{\mathcal{P}_2\mathcal{P}_2^*}$. For the case of the $X_z$ exciton we have

$$\mathcal{P}_1=\frac{2a^3}{\sqrt{d_1d_2}}\left[4\left(\frac{d_1}{d_2}\right)\frac{t_{13}^z}{\gamma_{X_z}t_{44}^z}U_\Gamma+\left(\frac{a}{d_1}\right)\frac{1}{\gamma_ht_{22}^h}U_X\right], \tag{13}$$

$$\mathcal{P}_2=\frac{2a^2}{\sqrt{d_1d_2}}\left[8\left(\frac{d_1}{d_2}\right)\frac{t_{13}^z}{t_{44}^z}U_\Gamma+\frac{2\pi ia}{t_{22}^hd_1}\times\left(\frac{1}{t_{44}^z\gamma_{X_z}d_2}-\frac{1-t_{22}^h}{t_{22}^h\gamma_hd_1}\right)U_X\right]\eta(\xi)\tilde{\xi}(0),$$

so that

$$\bar{w}=\frac{4\Lambda a^6}{d_1d_2}\left[4\left(\frac{d_1}{d_2}\right)\frac{t_{13}^z}{\gamma_{X_z}t_{44}^z}U_\Gamma+\left(\frac{a}{d_1}\right)\frac{1}{\gamma_ht_{22}^h}U_X\right]^2, \tag{14}$$

$$\sigma^2=\frac{2\Lambda a^4\bar{w}}{d_1d_2}\left[64\left(\frac{d_1}{d_2}\right)^2\frac{t_{13}^{z\,2}}{t_{44}^{z\,2}}U_\Gamma^2+\left(\frac{2\pi a}{t_{22}^hd_1}\right)^2\times\left(\frac{1}{t_{44}^z\gamma_{X_z}d_2}-\frac{1-t_{22}^h}{t_{22}^h\gamma_hd_1}\right)^2U_X^2\right]\tilde{W}(0).$$

The first terms in the square brackets can be interpreted as an electron conversion from the $X$ valley of AlAs to the $\Gamma$ valley of GaAs followed by the electron-hole recombination; they are small, since $t_{13}^z\ll1$. The other terms are due to indirect electron-hole recombination;[12] they occur only at the interface and, therefore, have a small factor $a/d_{1,2}$. This factor is not so small in short-period superlattices where $d_{1,2}$ are as large as a few lattice constants. The indirect electron-hole recombination prevails in such structures, if $a/d_{1,2}\gg t_{13}^z$. We omit the terms that contain both these factors or $|1-t_{44}^z|\ll1$.

The question arises of how small $|\mathcal{P}_1|$ should be in order to hold Eq. (1)? This is possible if the deviation of $|\mathcal{P}_2|^2$ from its average value in Eq. (10) essentially exceeds $|\mathcal{P}_1\mathcal{P}_2^*|$, i.e., when $|\mathcal{P}_1|^2\ll(h/l)^2|\mathcal{P}_2|^2$ or

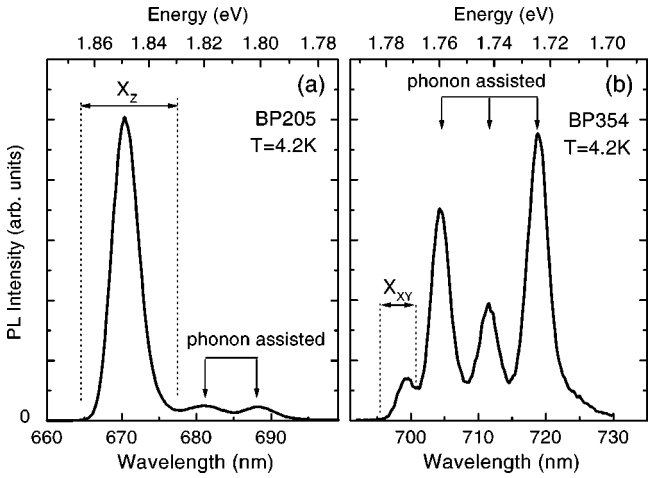


FIG. 2. The steady-state PL spectra of (a) an $X_z$ superlattice (sample BP205) and (b) an $X_{xy}$ superlattice (sample BP354) at a temperature of 4.2 K. The no-phonon lines included in the analysis of the PL decay are delimited by the dashed lines.

$$\frac{\overline{w^2}}{\sigma^2} \ll \frac{h^2}{l^2}. \tag{15}$$

### III. KINETICS OF EXCITON LUMINESCENCE IN TYPE-II GaAs/AlAs SUPERLATTICES. EXPERIMENT

The undoped GaAs/AlAs type-II superlattices used in this study were grown by molecular-beam epitaxy at 600 °C on (100) GaAs substrates. The sample BP205, in which the $X_z$ excitons were studied, contains 40 periods of 19.8 Å GaAs/25.5 Å AlAs each. The $X_{xy}$ excitons were studied in the sample BP354 which contains 25 periods of 25 Å GaAs/83.5 Å AlAs each. The samples were immersed in liquid helium during the measurements.

The steady-state photoluminescence (PL) was excited by an $Ar^+$ laser with a wavelength of 488 nm. The excitation power density was 50 W/cm$^2$. The time-resolved photoluminescence of $X_z$ excitons, which exhibits decays on the microsecond time scale, was excited by a *Q*-switched frequency-doubled Nd-doped yttrium aluminum garnet laser with a wavelength of 532 nm, a pulse duration of 0.15 $\mu$s, and a peak power density of 1.5 kW/cm$^2$. A nitrogen laser with a 337 nm wavelength, a pulse duration of 7 ns, and a peak power density of 2.5 kW/cm$^2$ was used to study the time-resolved photoluminescence of $X_{xy}$ excitons exhibiting millisecond-scale decays. The luminescence was analyzed by a double-grating monochromator equipped with a cooled photomultiplier operating in the photon-counting mode. The PL decay curves were recorded by a setup comprising two time-to-digital converters covering the delay range from nanoseconds to milliseconds. Sets of PL decay curves were measured across the excitonic PL wavelength ranges in each sample in order to obtain the time-resolved PL spectra, and to separate the decay of the no-phonon lines.

Figure 2 shows the steady-state PL spectra of the samples BP205 [Fig. 2(a)] and BP354 [Fig. 2(b)]. The $X_z$ exciton line with an energy $E_{ex}=1.849$ eV and its phonon replicas 29 and 48 meV below are seen in the spectrum of BP205, in agreement with the data of Ref. 13. The width of the lines in this sample does not exceed 12 meV. The $X_{xy}$ exciton line with an energy $E_{ex}=1.771$ eV and three phonon replicas with energies 12, 29, and 47 meV are seen in the spectrum of BP354. The width of the lines in this sample does not exceed 8 meV.

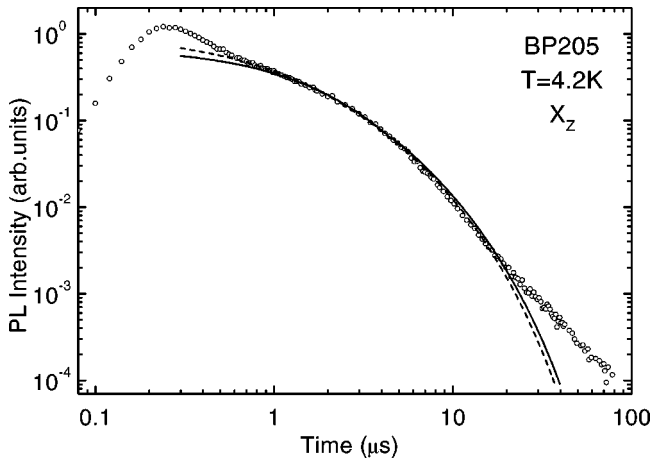


FIG. 3. Temporal evolution of the $X_z$ exciton emission. The theoretical curves (dashed and solid lines) were derived from Eqs. (1) and (12), respectively. The dots show the experimental data.

Figures 3 and 4 present the experimental results on the excitonic PL decay together with theoretical curves derived from Eqs. (1) and (12). It should be noted that our model (as well as that of Ref. 1) is valid only at large enough delay times when nonlinear in charge density terms can be omitted. For this reason we do not include the initial parts of the PL curves into consideration here (Figs. 3 and 4). The values of the parameters used in the calculation that ensured the best fit were $w_0=320c^{-1}$, $w_r=0.002\times10^6c^{-1}$, $\overline{w}=0.1\times10^6c^{-1}$, and $\sigma=0.61\times10^6c^{-1}$. We see that Eq. (1) fits the experimental data for the decay rates of $X_{xy}$ excitons in the sample BP354, whereas Eq. (12) is more appropriate for $X_z$ excitons in the sample BP205. Note that the value of

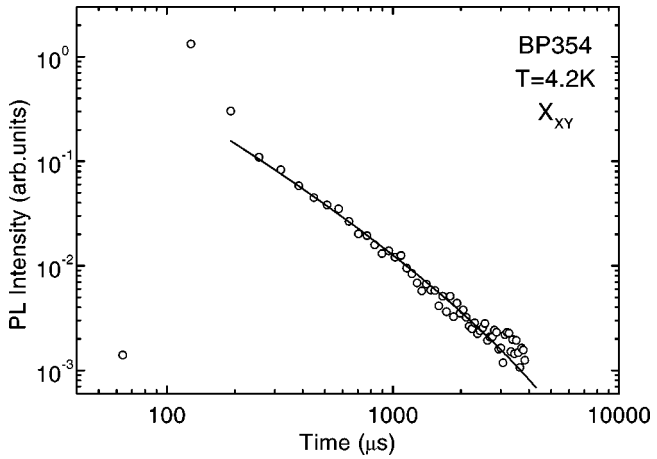


FIG. 4. Temporal evolution of the $X_{xy}$ exciton emission. The theoretical curve (solid line) was derived from Eq. (1). The dots show the experimental data.

$w_0$, which could be associated with the phonon-assisted recombination, is small in both curves. That is really the case at a low temperature. Recombination of $X_{xy}$ excitons is considerably slower than that of $X_z$ excitons. This means that the interfaces in our samples are perfect enough to apply our theory for interpretation of the experimental data.

Note that both theoretical curves do not fit the experimental data at the very large delay times $t \gg 1/\overline{w}$. The reason for that is the exponental factor $\exp(-\overline{w}t)$ which arises due to the $X_z$ exciton recombination at the plane interface. To explain the luminescence tail at the large delays, we have to involve some mechanism of the $X_z$ exciton creation at such times. If the number of the $X_z$ excitons arisen due to this mechanism $n(t)$ is independent of the random variable $w$, then the luminescence intensity is $I(t) \propto \overline{w}\, n(t)$ [see the reasoning after Eq. (10)], i.e., its kinetics follows the time dependence of $n(t)$.

The possible mechanism of the $X_z$ exciton creation can be associated with the $X_{xy}$ excitons, which also have to be excited in our experiments. The energy of the electrons at the bottom of the $X_{xy}$ valley is about 0.2 eV higher than that of the $X_z$ valley. Along with the radiative recombination, the electron transitions to the $X_z$ valley should occur due to the interface roughness. These transitions are similiar to that considered in Sec. II B for the $X_{xy}$ exciton recombination. Hence, the time dependence of the $X_z$ exciton number at the large delay times $t \gg 1/\overline{w}$ obey Eq. (1). Indeed, the power dependence $t^{-3/2}$, which follows from this equation, fits the tail of the experimental curve in Fig. 3.

Expressions (11)–(14) allow us to estimate the function $\tilde{W}(k)$ at the points $k=0$ and $k=2\pi/a$ only, which is not sufficient to determine the function. However, it is possible to estimate the parameters of the rough interface if we restrict ourselves to a particular type of the correlation function. We assume the exponential correlation function

$$W(\rho) = h^2 \exp(-\rho/l), \tag{16}$$

where $l$ is the correlation length. This type of the correlation function is more appropriate to our model of the rough interface (Fig. 1); it allows one to construct the two-position distribution, so that the distribution of slopes has a $\delta$ singularity, i.e., the slope is always zero except for a set of points (like point 1) with measure zero.[14] This is impossible for the Gaussian correlation function $W(\rho) = h^2 \exp(-\rho^2/l^2)$ most frequently employed in theoretical discussions.[15] The Fourier transform of the exponential function is

$$\tilde{W}(k) = \frac{2\pi h^2 l^2}{(1+k^2 l^2)^{3/2}}. \tag{17}$$

Unlike the Gaussian function, it has no exponential prefactor, decaying rapidly at a large $k$. This is also due to the singular points 1; only in the vicinity of these points is the momentum relaxation of indirect $X_{xy}$ excitons possible.

If we assume that the correlation functions are equal for the interfaces of both our samples, then the substitution of Eq. (17) into Eqs. (11) and (14) allows us to find the values of $h$ and $l$. The decay parameters of the wave functions $\gamma_{X_z, X_{xy}, h}$ in these expressions are determined by Eq. (7) for the known energies of the electrons or holes. As regards $U_{\Gamma,X}$, these values can be estimated only from the band-structure calculations for GaAs and AlAs. However, the first terms in the expression for $\overline{w}$ and $\sigma^2$ (14) can be omitted. Indeed, $t_{13}^z = t_{\Gamma X} m_\Gamma^{\mathrm{GaAs}}/(m_e a \gamma^r) < 0.06$, whereas $a/d_1 = 2/7$, i.e., the indirect recombination of $X_z$ exitons at the interface prevails in our samples. Then the values of $\sigma^2/\overline{w}^2$ and $w_r/\overline{w}$, which are determined from experimental data, become independent of $U_{\Gamma,X}$. For our experiments this estimation yields

$$\frac{\sigma^2}{\overline{w}^2} = \frac{1}{2}\left(\frac{2\pi}{a}\right)^2 \left(\frac{\gamma_h}{\gamma_{X_z} d_2} - \frac{1-t_{22}^h}{t_{22}^h d_1}\right)^2 \tilde{W}(0), \tag{18}$$

$$\frac{w_r}{\overline{w}} = \frac{4\pi^4 \gamma_h^2 t_{22}^{h\,2} d_1^{X_{xy}3} d_2^{X_{xy}}}{a^4 d_1^{X_z 3} d_2^{X_z 3}} \left[\frac{(1-t_{22}^h)^2}{\tilde{\gamma}_{X_{xy}}^4} + \frac{(1-t_{22}^{xy})^2}{\tilde{\gamma}_h^4}\right] \tilde{W}\left(\frac{2\pi}{a}\right).$$

Here $d_1^{X_z}$, $d_2^{X_z}$, $d_1^{X_{xy}}$, and $d_2^{X_{xy}}$ are the widths of GaAs and AlAs layers in the samples BP205 ($d_1^{X_z}$, $d_2^{X_z}$) and BP354 ($d_1^{X_{xy}}$, $d_2^{X_{xy}}$), where $X_z$ and $X_{xy}$ excitons were studied,

$$\gamma_{X_z} = \frac{1}{\hbar}\sqrt{2m_{Xl}^{GaAs}\left[E_X^{GaAs} - E_X^{AlAs} - \frac{\hbar^2}{2m_{Xl}^{AlAs}(d_2^{X_z})^2}\right]},$$

$$\gamma_h = \frac{1}{\hbar}\sqrt{2m_{hh}^{AlAs}\left[E_h^{GaAs} - E_h^{AlAs} - \frac{\hbar^2}{2m_{hh}^{GaAs}(d_1^{X_z})^2}\right]},$$

$$t_{22}^h = \frac{m_{hh}^{AlAs}}{m_{hh}^{GaAs}},$$

$$\tilde{\gamma}_{X_{xy}} = \frac{1}{\hbar}\sqrt{2m_{Xt}^{GaAs}\left[E_X^{GaAs} - E_X^{As} - \frac{\hbar^2}{2m_{Xt}^{AlAs}(d_2^{X_{xy}})^2}\right]},$$

$$t_{22}^{xy} = \frac{m_{Xt}^{AlAs}}{m_{Xt}^{GaAs}},$$

$$\tilde{\gamma}_h = \frac{1}{\hbar}\sqrt{2m_{hh}^{AlAs}\left[E_h^{GaAs} - E_h^{AlAs} - \frac{\hbar^2}{2m_{hh}^{GaAs}(d_1^{X_{xy}})^2}\right]},$$

$$\gamma^r = \frac{1}{\hbar}\sqrt{2m_\Gamma^{AlAs}(E_\Gamma^{AlAs} - E_X^{AlAs})}.$$

$E_{\Gamma,X,h}^{GaAs,AlAs}$ are the positions of the band extrema in GaAs and AlAs, $m_\Gamma^{GaAs}$ is the effective mass of the $\Gamma$ valley of GaAs, $m_{Xl,Xt}^{GaAs,AlAs}$ are the longitudinal and transversal effective masses in the $X$ valleys of GaAs and AlAs, $m_{hh}^{GaAs,AlAs}$ are longitudinal effective masses of heavy holes in GaAs and AlAs, and $m_e$ is the mass of the free electron. We assume $t_{21}^h \ll \gamma_h \sim 2/a$; this is the result of calculations of Ref. 7.

Equation (18) estimates the values of $\tilde{W}(0) = 2\pi h^2 l^2$ and $\tilde{W}(2\pi/a) \approx a^3 h^2/(4\pi^2 l)$. For the height $h$ and diameter $L$ [$L = 4l$ for the distribution (16)] (Ref. 14) of the roughnesses

we find $h \approx 1.25a$ and $L \approx 9a$. This is in agreement with the results of the structural studies of the GaAs/AlAs interface where the steps with a height $h=a/2$ and a mean length of 40–200 Å were observed (see Ref. 9 for a review). The steps with the mean height of about a few lattice constants and the diameter of about 50 Å have been observed by Raman spectroscopy[16] and photoelectrical spectroscopy.[17]

The rough estimate of the $h$ and $l$ values also can be done if we assume that the criterium (15) holds. This justifies Eq. (1) for $X_z$ excitons where $w_0 \equiv w_0^{X_z} = \Lambda |\mathcal{P}_1|^2$ and $w_r \equiv w_r^{X_z} = \Lambda |\mathcal{P}_2|^2$. Using Eq. (13), we find the expressions for $2w_r^{X_z}/w_0^{X_z}$ and $w_r/w_0^{X_z}$ [unlike $w_r^{X_z}$, the $w_r$ value corresponds to the $X_{xy}$ excitons (Fig. 4) and is determined by Eq. (11)]. These expressions accept the form of Eq. (18) after the substitutions $\sigma^2/\overline{w^2} \to 2w_r^{X_z}/w_0^{X_z}$ and $w_r/\overline{w} \to w_r/w_0^{X_z}$ of their left sides. The values of $w_0^{X_z} = 0.11 \times 10^6\, c^{-1}$ and $w_r^{X_z} = 0.38 \times 10^6\, c^{-1}$ ensure the best fit of the dashed line (Fig. 3) to the experimental data. This estimation yields $h=a$, $L=8.8a$, which are close to the values obtained from Eq. (12). For this reason both the theoretical curves (Fig. 3) fit the experimental data at small delay times. Nevertheless, Eq. (12) better fits the experimental data at large delay times where it ensures the slower decay of the luminescence: $I(t) \propto \exp(-\overline{w}t)/t$, instead of $I(t) \propto \exp(-w_0 t)/t^{3/2}$, as is predicted by Eq. (1).

## IV. DISCUSSION

In this paper we investigate the exciton luminescence in type-II GaAs/AlAs superlattices. We use the envelope-function approximation to consider the exciton recombination at an interface. To justify this approach, we have to note that the envelope-function approximation has been used only to find the reflection and transmission coefficients, while the Bloch functions $f_e$ and $f_h$ have been used to find the probability of the exciton recombination. An error arises only when we consider the Bloch amplitudes $u_\Gamma(\mathbf{r})$, $u_X(\mathbf{r})$, and $v(\mathbf{r})$ as periodical functions at the interface. Indeed, the deviation of these amplitudes from their bulk values is appreciable only at a small distance from the interface; this deviation is especially small at the interfaces of similar materials (e.g., GaAs/AlAs).[7,18]

It seems the boundary conditions (4) connect too few valleys of the electron spectrum to consider the interface influence on the exciton recombination; however, this is not the case. Indeed, the electron wave functions in the valleys that are not explicitly involved in Eq. (4) are strongly localized at the interface. This allows us to consider them in terms of the boundary conditions where the parameters $t_{ik}$ are influenced by these valleys. This procedure had been described when Eq. (4) was derived. The error arises only when these parameters are considered as independent of the electron energy; this is possible if the energy differences between the bottoms of the appropriate valleys considerably exceed the exciton energy. Note that a lot (about 10) of the electron bands are sometimes taken into account when the parameters of the interface matrix are calculated.[20]

We use the boundary conditions for the envelope wave function to consider the $\Gamma$-$X$ mixing of electrons at the interface. This approach is more general than the kinetic model proposed in Ref. 19. The kinetic equation where the electron states in the $\Gamma$ and $X$ valleys are considered as independent can be used for a small $\Gamma$-$X$ mixing. Only in that case is it possible to add the probabilities for the electron to be in $\Gamma$ and $X$ valleys. It should be noted that we also assume the small value of $\Gamma$-$X$ mixing ($|t_{13}^z| \ll 1$). However, this approximation is not principal for our consideration; it only makes the results [Eqs. (7), (11), (14), and (18)] not so cumbersome.

The influence of a nonstochastic process on the exciton recombination in Ref. 1 is taken into account by the exponential factor $e^{-w_0 t}$. This factor could be obtained if we insert the corresponding term in the $\tau$ approximation into the kinetic equation for the exciton density. If the $\tau$ approximation is not applicable for the process, then this factor becomes nonexponential.[3] A correlation between stochastic and nonstochastic processes changes the second factor in Eq. (1). In this case the probability of the exciton recombination $w$ is not a simple sum of the probabilities of each process. As a result, the additional terms arise in the expression for $w$ [the second and third terms in Eq. (10)]. These terms are linear in the stochastic variable, so that their averages vanish. For this reason they are not important when the mean intensity of the luminescence or the light absorption[6] is considered. However, they are important for the kinetic phenomena because they determine the mean square of the deviation $\sigma$ of the stochastic variable from its mean value. The nonexponential behavior of the decay rate (12) holds any time when the linear terms with respect to the stochastic variable are dominating in the expression for $w$. Such a situation can occur also in other type-II semiconductor structures where the interface influence is essential, e.g., in quantum dots.[21]

Expressions (11) and (14) relate the parameters of the radiative decay rates ($w_r, \overline{w}$, and $\sigma$) with the correlation function of the rough interface. The values of the Fourier transform of this function only at two particular points, $k=0$ and $k=2\pi/a$, are important for these relationships. This allows one to estimate the parameters only for simplest functions [like Eq. (16)]. The real interface might be more complicated. In particular, the rough interface could be characterized by a few different scales. Expressions (11) and (14) take into account all the scales; however, it is impossible to determine more than two parameters simultaneously from the time-resolved luminescence experiments.

Comparing the experimental results (Figs. 3 and 4), we see that the mean lifetime of $X_{xy}$ excitons essentially exceeds that of $X_z$ excitons. This happens due to the recombination of the $X_z$ excitons at a plane interface. Meanwhile, the influence of the roughnesses, i.e., the nonexponential factor in $I(t)$, is more essential for the $X_z$ excitons. This becomes clear from our analysis. Indeed, $\sigma \propto \tilde{W}(0)$, whereas $w_r \propto \tilde{W}(2\pi/a)$ while $\tilde{W}(2\pi/a) \ll \tilde{W}(0)$. The recombination occurs in some region near a step (point 1 in Fig. 1). The size of this region is of the order of $|\mathbf{q}_\parallel|^{-1}$, where $\mathbf{q}_\parallel$ is the parallel-to-interface component of the electron wave vector. This region is large for the $X_z$ electrons ($|\mathbf{q}_\parallel| \simeq r_B^{-1}$, where $r_B$ is the exciton radius), but it is small for the $X_{xy}$ electrons ($|\mathbf{q}_\parallel| \simeq 2\pi/a$). As a

result, the small factor [of the order of $(a/l)^3$] arises in the expression for $w_r$.

In conclusion, the kinetics of the type-II exciton luminescence at a rough interface has been investigated both theoretically and experimentally. The Klein *et al.* law (1) is shown to be valid for the decay rate of $X_{xy}$ excitons, whereas the more complicated expression (12) is applicable for $X_z$ excitons. Expressions (11) and (14), which relate the parameters of the exciton kinetics to the statistical characteristics of the rough interface, allow us to estimate some of these characteristics from the experimental data. The values of the mean height of 7 Å and the length of 50 Å of the roughnesses obtained from our experiments are in good agreement with the results of the structural investigations of the GaAs/AlAs interface.


## ACKNOWLEDGMENTS

Authors wish to thank Professor E. L. Ivchenko and Professor V. L. Al'perovich for valuable discussions. This work was supported by the Russian Foundation for the Basic Research, Grants Nos. 99-02-17019, 98-02-17896, 00-02-17658, and the Program ''Physics of Solid State Nanostructures'' by the Russian Interdisciplinary Scientific and Technical Council, Grant No. 99-1133.


## APPENDIX A: DERIVATION OF EQ. (5)

To obtain Eq. (5a), let us write the boundary conditions (4a) at the plane $z=\xi$:

$$\Psi^r_{Xz}(\xi)=\Psi^l_{Xz}(\xi), \tag{A1}$$

$$\partial_z\Psi^r_{Xz}(\xi)=t^z_{41}\eta(\xi)\Psi^l_\Gamma(\xi)+t^z_{44}\partial_z\Psi^l_{Xz}(\xi),$$

$$\Psi^l_\Gamma(\xi)+t^z_{12}\partial_z\Psi^l_\Gamma(\xi)+t^z_{13}\eta(\xi)\Psi^l_{Xz}(\xi)=0.$$

$$\Psi^{l,r}_{\Gamma,Xz}(\xi)\approx\Psi^{l,r}_{\Gamma,Xz}(0)+\xi\partial_z\Psi^{l,r}_{\Gamma,Xz}(0),$$

$$\partial_z\Psi^{l,r}_{\Gamma,Xz}(\xi)\approx\partial_z\Psi^{l,r}_{\Gamma,Xz}(0)+\xi\partial^2_{zz}\Psi^{l,r}_{\Gamma,Xz}(0).$$

The factor $\eta(\xi)=\exp(2\pi i\xi/a)$ takes two values $\pm1$ for $\xi=a$ or $\xi=a/2$, respectively. It was introduced to consider the symmetry properties of the Bloch functions with respect to translation by a single monomolecular layer $(a/2)$ along the $z$ axis.[10] The inequality $|\xi\Psi'|\sim h/\lambda\ll1$ allows us to assume

$$\Psi^{l,r}_{\Gamma,Xz}(\xi)\approx\Psi^{l,r}_{\Gamma,Xz}(0)+\xi\partial_z\Psi^{l,r}_{\Gamma,Xz}(0),$$

$$\partial_z\Psi^{l,r}_{\Gamma,Xz}(\xi)\approx\partial_z\Psi^{l,r}_{\Gamma,Xz}(0)+\xi\partial_z\Psi^{l,r}_{\Gamma,Xz}(0).$$

The last term in the second equation can be omitted, since $\partial^2_{xx}\Psi^{l,r}_{\Gamma,Xz}=-k^2\Psi^{l,r}_{\Gamma,Xz}\to0$ when $k\to0$. Then from Eq. (A1) we obtain

$$\Psi^r_{Xz}+\xi\partial_z\Psi^r_{Xz}=\Psi^l_{Xz}+\xi\partial_z\Psi^l_{Xz},$$

$$\partial_z\Psi^r_{Xz}=t^z_{41}\eta(\xi)(\Psi^l_\Gamma+\xi\partial_z\Psi^l_\Gamma)+t^z_{44}\partial_z\Psi^l_{Xz},$$

$$\Psi^l_\Gamma+(t^z_{12}+\xi)\partial_z\Psi^l_\Gamma+t^z_{13}\eta(\xi)(\Psi^l_{Xz}+\xi\partial_z\Psi^l_{Xz})=0,$$

where $\Psi^{l,r}_{\Gamma,Xz}\equiv\Psi^{l,r}_{\Gamma,Xz}(0)$. The substitution of $\partial_z\Psi^r_{Xz}$ from the second equation into the first one leads to Eq. (5a). Equations (5b) and (5c) can be obtained from Eqs. (4b) and (4c) in the same manner.

## APPENDIX B: DERIVATION OF EQ. (7)

First of all, note that $\Psi^{l,r}_\Gamma\propto\eta(\xi)$ and $\varphi^{l,r}_\Gamma\propto\eta(\xi)$, i.e., the factors $\eta(\xi)$ in Eqs. (5a) disappear after the substitutions $\Psi^{l,r}_\Gamma\to\eta(\xi)\Psi^{l,r}_\Gamma$ and $\varphi^{l,r}_\Gamma\to\eta(\xi)\varphi^{l,r}_\Gamma$. To obtain the boundary conditions for $\Psi^{l,r}_{\Gamma,Xz}$ and $\varphi^{l,r}_{\Gamma,Xz}$ we substitute these envelopes from Eq. (6) into Eqs. (5a). If we average these equations and then subtract the average equations from the initial ones, we obtain

$$\Phi^r_{Xz}=-t^z_{41}\overline{\xi\varphi^l_\Gamma}+\Phi^l_{Xz}+(1-t^z_{44})\overline{\xi\partial_z\varphi_{Xz}}, \tag{B1}$$

$$\partial_z\Phi^r_{Xz}=-t^z_{41}\Phi^l_\Gamma+t^z_{41}\overline{\xi\varphi^l_\Gamma}+t^z_{44}\partial_z\Phi^l_{Xz},$$

$$\Phi^l_\Gamma+t^z_{12}\partial_z\Phi^l_\Gamma+\overline{\xi\partial_z\varphi^l_\Gamma}+t^z_{13}\Phi^l_{Xz}+t^z_{13}\overline{\xi\partial_z\varphi^l_{Xz}}=0,$$

$$\varphi^r_{Xz}=-t^z_{41}\xi\Phi^l_\Gamma+\varphi^l_{Xz}+(1-t^z_{44})\xi\partial_z\Phi^l_{Xz},$$

$$\partial_z\varphi^r_{Xz}=-t^z_{41}\varphi^l_\Gamma+t^z_{41}\xi\partial_z\Phi^l_\Gamma+t^z_{44}\partial_z\varphi^l_{Xz},$$

$$\varphi^l_\Gamma+t^z_{12}\varphi^l_\Gamma+\xi\partial_z\Phi^l_\Gamma+t^z_{13}\varphi^l_{Xz}+t^z_{13}\xi\partial_z\Phi^l_{Xz}=0.$$

We write the envelopes $\Phi^{l,r}_{\Gamma,Xz}$ and $\varphi^{l,r}_{\Gamma,Xz}$ in the form (7) and substitute them into Eqs. (B1). The last three equations (B1) allow one to express the diffuse components $\varphi^{l,r}_{\Gamma,Xz}$ as functions of $\xi$, $R_{Xz}$, and $T_{\Gamma,Xz}$. The reflection $(R_{Xz})$ and transmission $(T_{\Gamma,Xz})$ coefficients can be obtained then from the first three equations (B1).

To simplify the expressions for $R_{Xz}$, $T_{\Gamma,Xz}$, and the amplitudes $A^l_{\Gamma,Xz}$, we assume $ap\ll1$, $aq\ll1$ and use the relationships between the matrix elements (4). We also assume the mean height of the roughnesses to be small $h\ll l$, $hp\ll1$, $hq\ll1$, so that it is possible to omit the $\xi$-dependent terms from the first three equations (B1). Such simplifications are not principal; they only make the expressions for $R_{Xz}$, $T_{\Gamma,Xz}$, and $A^l_{\Gamma,Xz}$ not too cumbersome. A more general case has been considered in Ref. 6. It has been shown that the $\xi$-dependent terms in the first three Eqs. (B1) result in effective changes in the matrix elements $t_{ik}$ which are small when $h/l\ll1$. The expressions for the $R_{Xxy,h}$, $T_{Xxy,h}$, and $A^{l,r}_{Xxy,h}$ for the electrons in $X_{xy}$ valleys and the holes were obtained from Eqs. (5b) and (5c) in the same manner.

*Electronic address: brag@isp.nsc.ru


[1] M. V. Klein, M. D. Sturge, and E. Cohen, Phys. Rev. B **25**, 4331 (1982).

[2] F. Minami, K. Hirata, K. Era, T. Yao, and Y. Masumoto, Phys. Rev. B **36**, 2875 (1987).

[3] I. N. Krivorotov, T. Chang, G. D. Gilliland, L. P. Fu, K. K. Bajaj, and D. J. Wolford, Phys. Rev. B **58**, 10 687 (1998).

[4] S. Nagao, K. Fujii, T. Fujimori, H. Gotoh, H. Ito, and F. Minami,

J. Cryst. Growth **175**, 10 687 (1997); B. A. Wilson, Carl E. Bonner, R. C. Spitzer, F. Fisher, P. Dawson, K. J. Moore, C. T. Foxon, and G. W.'t Hooft, Phys. Rev. B **40**, 1825 (1989); E. Finkman, M. D. Sturge, M.-H. Meynadier, R. E. Nahory, M. C. Tamargo, D. M. Hwang, and C. C. Chang, J. Lumin. **39**, 57 (1987); B. A. Wilson, Carl E. Bonner, R. C. Spitzer, P. Dawson, K. J. Moore, and C. T. Foxon, J. Vac. Sci. Technol. B **6**, 1156 (1988).

[5] E. L. Ivchenko and G. E. Pikus, *Superlattices and Other Heterostructures. Symmetry and Optical Phenomena*, 2nd ed. (Springer-Verlag, Berlin, 1997).

[6] L. Braginsky, Physica E **5**, 142 (1999).

[7] T. Ando and H. Akera, Phys. Rev. B **40**, 11 619 (1989).

[8] D. Lüerßen, A. Oehler, R. Bleher, and H. Kalt, Phys. Rev. B **59**, 15 862 (1999).

[9] F. Bechstedt and R. Enderlein, *Semiconductor Surfaces and Interfaces. Their Atomic and Electronic Structures* (Akademie-Verlag, Berlin, 1988).

[10] I . L. Aleiner and E. L. Ivchenko, Fiz. Tech. Poluprovodn. **27**, 594 (1993) [Semiconductors **27**, 330 (1993)]; Y. Fu, M. Willander, E. L. Ivchenko, and A. A. Kiselev, Phys. Rev. B **47**, 13 498 (1993).

[11] F. G. Bass and I. M. Fuks, *Wave Scattering from Statistically Rough Surfaces* (Pergamon Press, New York, 1979).

[12] L. Braginsky, Phys. Rev. B **57**, R6870 (1998).

[13] D. Scalbert, J. Cernogora, C. Benoit á la Guillaume, M. Maaref, F. F. Charfi, R. Planel, Solid State Commun. **70**, 945 (1989).

[14] M. V. Berry, Philos. Trans. R. Soc. London, Ser. A **273**, 611 (1973); J. M. Ziman, *Models of Disorder. The Theoretical Physics of Homogeneously Disordered Systems* (Cambrige University Press, Cambridge, 1979).

[15] For the exciton problem this approximation has been used in V. A. Kosobukin, Fiz. Tverd. Tela **41**, 330 (1999) [Phys. Solid State **41**, 296 (1999)]; see also references therein.

[16] V. A. Gaisler, D. A. Tenne, N. T. Moshegov, A. I. Toropov, A. P. Shebanin, and A. L. Yaskin, Fiz. Tverd. Tela **38**, 2242 (1996) [Phys. Solid State **38**, 1235 (1996)].

[17] V. L. Al'perovich, N. T. Moshegov, V. V. Popov, A. S. Terehov, V. A. Tkachenko, A. I. Toropov, and A. S. Yaroshevich, Fiz. Tverd. Tela **39**, 2085 (1997) [Phys. Solid State **39**, 1864 (1997)].

[18] P. von Allmen, Phys. Rev. B **46**, 15 377 (1992).

[19] M. Maaref, E. F. Charfi, D. Scalbert, C. Benoit á la Guillaume, and R. Planel, Solid State Commun. **81**, 35 (1992).

[20] S. N. Grinyaev (private communication); see, e.g., S. N. Grinyaev and G. F. Karavaev, Fiz. Tverd. Tela **42**, 752 (2000) [Phys. Solid State **42**, 772 (2000)].

[21] A. O. Govorov and A. V. Chaplik, Zh. Éksp. Teor. Fiz. **99**, 1853 (1991) [Sov. Phys. JETP **72**, 1037 (1991)]; A. V. Kalameitsev, A. O. Govorov, and V. Kovalev, Pis'ma Zh. Éksp. Teor. Fiz. **68**, 634 (1998). [JETP Lett. **68**, 669 (1998)].